JOURNAL OF PROPULSION AND POWER
Vol. 13, No. 2, March–April 1997

Flow Analysis of a Solid Propellant Rocket Motor with Aft Fins

Bruno Chaouat*
ONERA, Chatillon BP 72 F 92322, France

Solid rocket motors often have a complex grain geometry, such as fins slots to optimize the ballistic performance. These shapes result in a complex three-dimensional flowfield that locally augments the propellant burning, nozzle ablation, and insulator erosion. This work solved a steady-state, three-dimensional inviscid flowfield for a complex internal geometry with 16 fins. For the computation, 1/16 of the motor geometry is simulated. The results predicted the presence of circumferential and swirl flow in the nozzle region. The distribution of the flowfield indicated the likelihood of nonsymmetric heat flux at the wall in this area. The specific mass flow rate in the fins are below the predicted levels that would induce erosive burnings.

Introduction

THE performance improvement of solid propellant rocket motors often requires complex internal geometry such as fins. For example, in the development of advanced solid rocket motor (ASRM) for the Space Shuttle, the geometry of the aft-end grain with fin slots must be carefully selected. For solid propellant rocket motors with this kind of complex geometry, the flowfield structure must be predicted to control the extent of erosive burning as well as the ablation of nozzle material and internal protection layers. This information is necessary to evaluate the effects on motor performance. This work represents a preliminary step for more complex simulations for a priori prediction of erosive burning and ablation of nozzle and thermal insulation materials.

Recently, much attention has been given to numerical simulation of internal aerodynamics inside solid rocket motors. Because of the recent progress in computing power, this field is developing rapidly. The numerical simulation of the internal flow in a motor usually involves a flow that ranges from the low subsonic to the supersonic regime. Johnston[1] presented the results of a numerical simulation of the internal three-dimensional inviscid flow in a Titan solid rocket motor upgrade (SRMU). The purpose of this simulation was to determine if the SRMU internal complex geometry could cause circumferential flows that might lead to joint O-ring erosion.

Another motivation to simulate the internal flow is to study the effect of propellant combustion under the influence of acoustic waves in a solid rocket motor. In this area, Tseng and Yang[2] solved the Navier–Stokes equations with chemical reactions in both gas and condensed phases.

In this article, the internal flowfield of the internal solid rocket motor with aft fins is simulated by means of the Euler equations. The inviscid flow simulation is a good approximation of the viscous/turbulent flow, since the physics of this type of flow are governed by the injection at wall. Another rationale for using Euler analysis is the limited requirements for computer resources. Nevertheless, the computer resources required by this study still appear to be quite large. The major archival contribution of this work is the description of flow processes in three-dimensional geometry. Nonuniform nozzle ablation and erosive burning in the fins are important issues of this large and complicated numerical simulation.

Conditions of Computation

The numerical scheme used in the computer program is a finite volume method with an explicit second-order centered scheme proposed by Ni.[3] The equations are directly discretized in the physical space. The boundary condition treatment is based on the utilization of compatibility relationships along characteristic lines, as described in detail by Cambier et al.[4] The code was calibrated against some simpler cases, in particular, with the shock-tube problem, called the Riemann problem in mathematical modeling. A good agreement with well-known solutions was observed by Chaouat.[5] More detailed information about the numerical method and boundary conditions can be found in Ref. 6.

Figure 1 presents the particular three-dimensional geometry studied in the present work. It is repesentative of an actual motor with aft fins. All 16 fins are evenly distributed. Three computational domains have been defined as indicated in Fig. 2: 1) the upstream cylindrical port, 2) the cavity region of a single fin, and 3) the aft chamber plus the exit nozzle. Subdomain 3 clearly indicates the finned region (from i = 1 to 30), the converging portion of the nozzle (from i = 30 to 76), the location of the nozzle throat (for i = 76), and the location

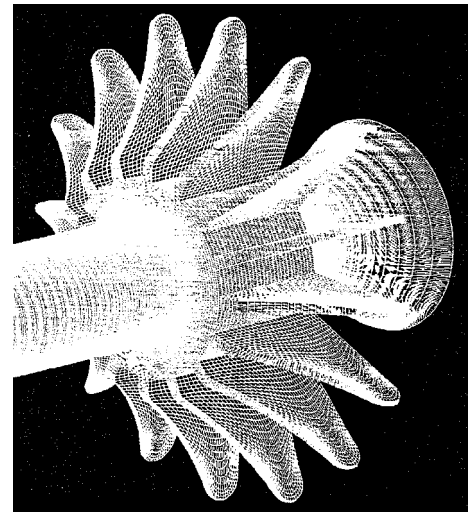

Fig. 1 View of three-dimensional geometry.

Presented as Paper 92-3507 at the AIAA 28th Joint Propulsion Conference and Exhibit, Nashville, TN, July 6–8, 1992; received Dec. 9, 1994; revision received May 5, 1996; accepted for publication June 14, 1996.

*Research Scientist, Energetics Department.

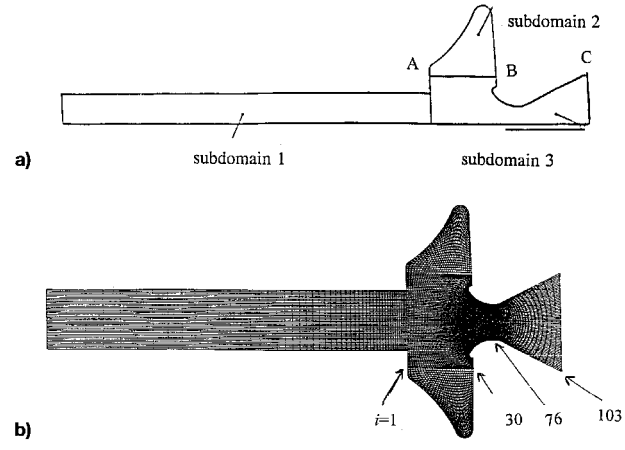

Fig. 2 a) Three subdomains considered in the numerical simulation and b) meshes of the three subdomains.

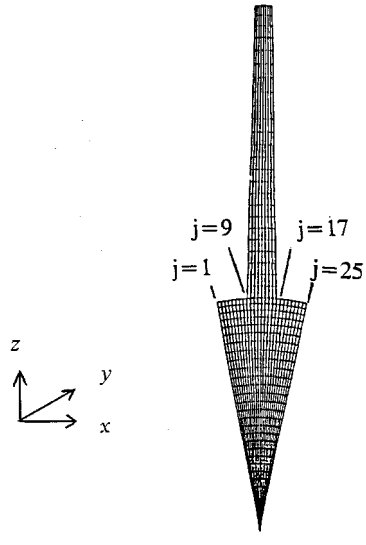

Fig. 3 Planar view of the mesh.

of the exit section (i = 103). For a motor geometry with 16 fins, the computational domain only needs to be 1/32 of the circumference in the azimuthal direction. However, this method was not chosen because of the periodicity of the geometry in the azimuthal direction. Indeed, 1/16 of the total motor circumference shown by Fig. 3 is needed to impose a complete symmetry in the computational domain.

Six types of boundary conditions are used in this application. On the injected wall, the propellant surface is burning. On the lateral boundaries, which limit the computational domain in the azimutal direction, a slip condition is applied. For the head end, there is a symmetry condition. At interfaces, a subdomain condition is applied. The exit plane is supersonic. Finally, axis conditions are imposed for r = 0. The number of points for each domain are, respectively, 26,250 (domain 1, 50 × 25 × 21); 6525 (domain 2, 29 × 9 × 25); and 79,825 (domain 3, 103 × 25 × 31). The total number of points is 112,600. The motor characteristics for the computation are a perfect gas constant of 275 J/kg K; a specific heat ratio of 1.14; a flame temperature of 3635 K; a burning rate of 11 mm/s; a density of propellant of 1815 kg/m^3; and a mean chamber pressure of 58.8 bar.

Numerical Results

Present results have been obtained after 94,400 iterations with a local time step. The Courant–Friedrich–Lewy number has been set to 0.6. Total computer time was 60 h on Cray 2 and the central memory requirement was 15 MW. Note that the code is vectorized and the time used per iteration per point is 19 μs of CPU.

Figure 4 shows the steady-state solution in the symmetry plane. Note that the pressure is almost uniform in the upstream duct and that a good continuity of the contour lines is observed at the domain interfaces.

Figure 5 reveals some interesting features of the flow by showing constant vorticity curves and velocity vectors in the cross section at two axial locations in the motor. This figure indicates the presence of circumferential flow and vortex shedding, which implies that the flow is not axisymmetric in the nozzle portion of the flow. This result provides some information applicable to other motors with aft fins. In particular, Waesche et al.[7] obtained the tendency of this type of flow with the cold air flow test on the ASRM motor. In the same way, Johnston[1] observed circumferential flows with numerical simulations in an SRMU. In the present calculation, notice that the flowfield presents a complete symmetry that is in good agreement with the conditions of computation. The computational results show that the maximum value of vorticity increases from the downstream duct to the nozzle converging part and decreases in the nozzle diverging part.

Figure 6 shows the profile of specific mass flow rate along the boundary ABC (i = 1 to 103) of Fig. 2 for each azimuthal plane (from j = 1 to 25), with the axial dimensionless distance that is defined as $x = x^*/l$, where x^* is the real distance and l is the complete axial length of the geometry. According to this definition, the nozzle exit is located at x = 1, since $x^* = l$. These figures show that the distribution of the mass flow rate is nonuniform in the converging part of the nozzle (from i = 40 to 76 of Fig. 2) and confirm the three-dimensional aspect of the flow. This three-dimensional nature can be traced back to the strong vortices that are generated when the flow from the fin merges with the core of the flow. This particular geometry of the flow is enhanced in the submerged nozzle converging part. The distribution of the flow should modify the convective heat flux density at the wall, such as indicated in Fig. 4 of Ref. 8. It could lead to nonuniform nozzle ablation in the azimuthal direction in the converging part. According

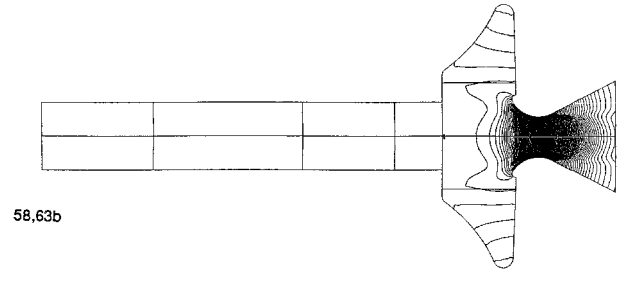

Fig. 4 Static pressure contours obtained in the symmetry plane (j = 13) ΔP = 0.15 bar.

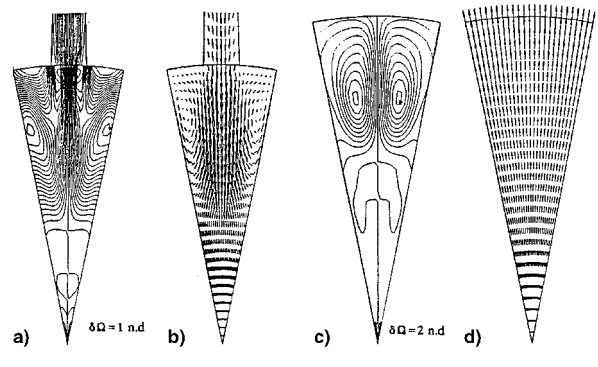

Fig. 5 Steady-state solution obtained in the cross section: a) constant vorticity curves in the section (i = 25), b) velocity vectors in the section (i = 25), c) constant vorticity in the nozzle exit plane (i = 103), and d) velocity vectors in the nozzle exit plane (i = 103).

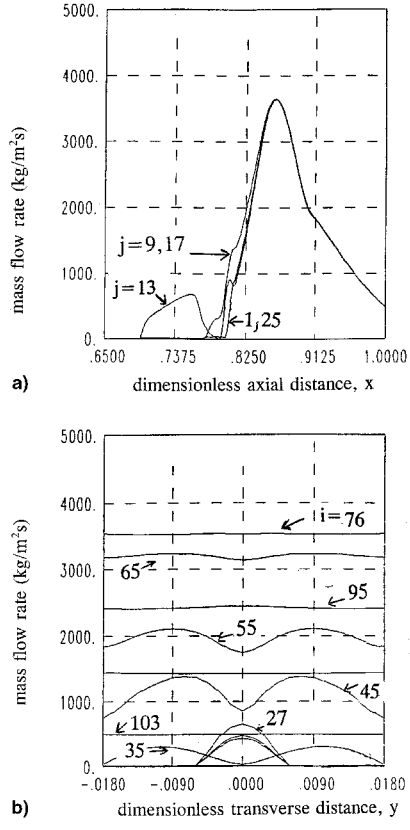

Fig. 6 Evolution of the specific mass flow rate (kg/m² s) along the frontier *ABC* of subdomain 3 with normalized coordinate in the a) longitudinal direction for different azimuthal planes and b) the transversal direction for different axial planes.

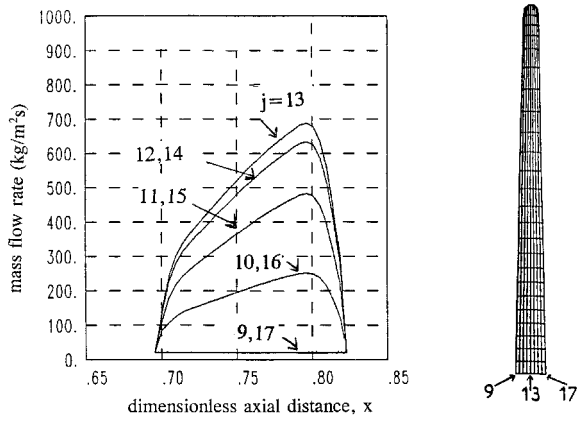

Fig. 7 Evolution of the specific mass flow rate (kg/m² s) along the frontier *AB* of subdomain 3 with normalized coordinate in the longitudinal direction for different azimuthal planes.

to Fig. 6b, the nonuniformity in the azimuthal direction vanishes quickly as the flow proceeds to the nozzle, where fairly uniform heat flux and ablation are expected. Furthermore, one must keep in mind that the computation represents the initial time of the propellant combustion, and it is well known that the aft fins disappear during the combustion.

Figure 7 shows the profile of the specific mass flow rate (kg/m²s) along the boundary *AB* of Fig. 2 for each azimuthal plane (from $j = 9$ to 17). It is known that the burning rate of a solid propellant depends mostly on the pressure, but can be modified when high mass flow rate sweeps the propellant surface (erosive burning). Erosive burning results from the interaction between the propellant burning characteristics and the flow, and is affected by the actual size of the motor according to Fig. 4 in Ref. 9. The motor characteristics (slab motor) that are given by the pressure $p = 57$ bar and the injected specific mass flow rate $m = 14.7$ kg/m²s are very close to the values for the solid rocket motor with aft fin. Since the thickness of the fin is of a few millimeters, there should not be any possibility for erosive burning in the fin, because the maximum specific mass flow rate (700 kg/m²s) is not high enough to induce erosive burning.

Conclusions

The computed internal flowfield clearly demonstrates the three-dimensional nature of the flow in the rocket motor. The one valuable insight that the solution provides is the influence of aft fins on the flowfield entering the nozzle. In particular, circumferential flows are observed off the fin at the entrance of the nozzle. A computation to evaluate the risks of erosive burning in the fins and of nozzle material ablation is reported with success. This work concludes that there should not be any possibility for erosive burning in the fins and predicted the possibility of a nonuniform ablation in the azimuthal direction limited to the first part of the converging portion of the nozzle.

Acknowledgments

This work was conducted at ONERA with financial support from Direction des Missiles et de l'Espace de la Direction Générale de l'Armement du Ministère de la Défense.

References

[1]Johnston, W. A., "A Computational Fluid Dynamics Analysis of the Internal Flow in a Titan SRMU," AIAA Paper 90-2079, July 1990.

[2]Tseng, I. S, and Yang, V., "Interactions of Homogeneous Propellant Combustion and Acoustic Waves in a Solid Rocket Motor," AIAA Paper 92-0101, Jan. 1992.

[3]Ni, R. H., "A Multiple-Grid for Solving the Euler Equations," *AIAA Journal*, Vol. 20, No. 11, 1982.

[4]Cambier, L., Dusson, F., and Veuillot, J. P., "Multi-Domain Method for the Euler Equations, Application to Subdomain with Overlapping," *La Recherche Aérospatiale*, No. 3, 1985, pp. 181–188.

[5]Chaouat, B., "Modélisation et Simulation des Écoulements Turbulents dans les Propulseurs à Propergol Solide," Ph.D. Dissertation, Paris 6 Univ., Paris, France, Oct. 1994.

[6]Chaouat, B., and Vuillot, F., "A Multi-Domain 3D Euler Solver for Flows in Solid Propellant Rocket Motor with Aft Fin," AIAA Paper 92-3507, July 1992.

[7]Waesche, R. H. W., Marchmhman, J. F., and Kuppa, S., "Effects of Grain and Aft-Dome Configuration on Aft-End SRB Internal Flows," *Journal of Propulsion and Power*, Vol. 7, No. 2, 1991, pp. 163–170.

[8]Borie, V., Brulard, J., and Lengelle, G., "Aerothermochimical Analysis of Carbon-Carbon Nozzle Regression in Solid-Propellant Rocket Motors," *Journal of Propulsion and Power*, Vol. 5, No. 6, 1989, pp. 665–673.

[9]Godon, J. C., Duterque, J., and Lengelle, G., "Erosive Burning in Solid Propellant Motors," *Journal of Propulsion and Power*, Vol. 9, No. 6, 1993, pp. 806–811.